LASER INTERFEROMETER GRAVITATIONAL WAVE OBSERVATORY
- LIGO -
CALIFORNIA INSTITUTE OF TECHNOLOGY
MASSACHUSETTS INSTITUTE OF TECHNOLOGY

Technical Note **LIGO-T1500320-v1** Date:09 June 2015

Advanced interferometers strategy on earthquake perturbations

Sebastien Biscans, Michael Coughlin, Jan Harms

California Institute of Technology
LIGO Project, MS 18-34
Pasadena, CA 91125
Phone (626) 395-2129
Fax (626) 304-9834
E-mail: info@ligo.caltech.edu

Massachusetts Institute of Technology
LIGO Project, Room NW22-295
Cambridge, MA 02139
Phone (617) 253-4824
Fax (617) 253-7014
E-mail: info@ligo.mit.edu

LIGO Hanford Observatory
Route 10, Mile Marker 2
Richland, WA 99352
Phone (509) 372-8106
Fax (509) 372-8137
E-mail: info@ligo.caltech.edu

LIGO Livingston Observatory
19100 LIGO Lane
Livingston, LA 70754
Phone (225) 686-3100
Fax (225) 686-7189
E-mail: info@ligo.caltech.edu

http://www.ligo.caltech.edu/

Contents

1 Introduction

Earthquakes are currently reducing the duty cycles of advanced interferometers due to the excess ground motion that they create. This document reports the different actions taken to understand, analyse and reduce the impact of earthquakes on interferometers, and especially on the LIGO interferometers. This work could be categorized in three main parallel actions.

1. Analysing different data sets to understand the behaviour of the LIGO interferometers during events (Section 2 and 3)
2. Implementing an earthquake monitor and warning system (Section 4)
3. Improving the interferometers behaviour during events (Section 5)

2 S5 and S6 data

A joint effort has been done to process and analyse the data from S5 and S6. The goal is to show the lock status of the interferometers during major earthquakes.

The lock status was not actually recorded in the S5/S6 frames, but only the state vector of the interferometers (second bit of H1:IFO-SV_STATE_VECTOR and L1:IFO-SV_STATE_VECTOR channels), which gives the same information. The earthquake arrival time is estimated by the 'earthquake monitor' (see Section 4), so we can correlate the lock losses with earthquakes.

2.1 Time series of the ground

During S5/S6, there was 191 major earthquakes (magnitude over 6). For each of them, we plotted the relative interferometers status for both LIGO sites [1].

These results allow us to do some rough statistics. In table 1, we assume that all the lock losses happening less than 4000 seconds after the arrival of the event are due to the event itself. 41.88% of the LLO data and 37.70% of LHO data are not exploitable because the interferometers were not locked at that time, but by looking at the exploitable data, we see that around 75% of the major earthquakes caused the interferometers to loose lock.

	LLO	LHO
Lock losses due to earthquakes	43.46 %	48.69 %
Unlock before the earthquakes arrival	41.88 %	37.70 %
No lock loss during the earthquake	14.66 %	13.61 %

Table 1: Behaviour of the interferometers during earthquakes

Among the lock losses, we have 3 categories.

- If the lock loss happened right at the earthquake arrival, I assume that the lock loss is due to P-waves.

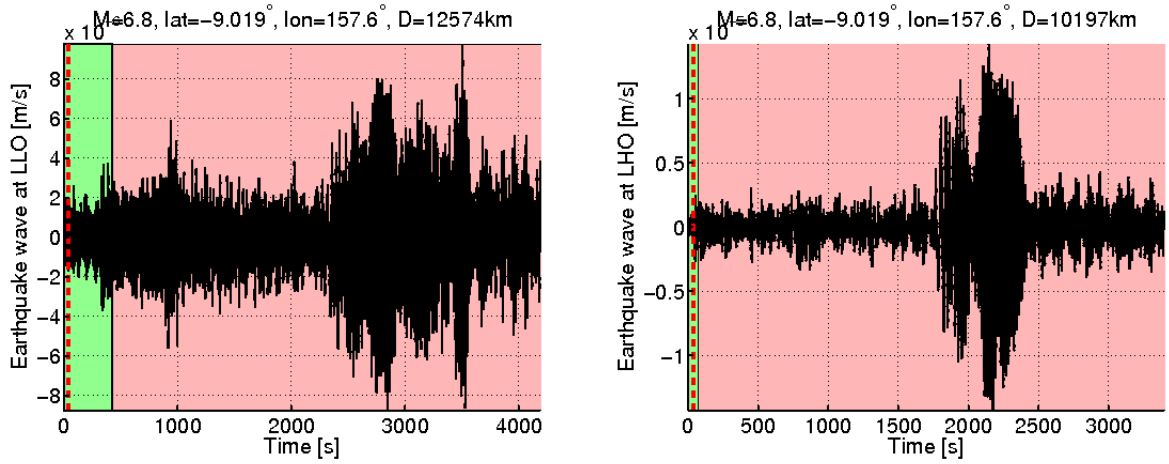

(a) Example for LLO

(b) Example for LHO

Figure 1: These plots display the time series of the seismometers in the horizontal direction for LLO and LHO. The vertical red dot line represents the arrival time of the event. The color background indicates the status of the state vector. Green means that the interferometer is locked, red means that it is unlock. A similar plot is generated for each event.

	LLO	LHO
Lock losses due to P-waves	15.66 %	73.12 %
Lock losses due to S-waves	59.04 %	15.05 %
Lock losses due to Rf-waves	25.30 %	11.83 %

Table 2: Behaviour of the interferometers during earthquakes

- If the lock loss happened in less than 1500 seconds after the earthquake arrival, we assume that the lock loss is due to S-waves.
- If the lock loss happened after 1500 seconds, we assume that the lock loss is due to Surface waves (Rayleigh waves).

As shown in Table 2, the behaviour seen at LLO and LHO is quite different: LLO seems to have most issues because of the S-waves arrivals, while LHO has most trouble with the P-wave arrivals. This might be due at the geographical position of each site (LHO is very close to Alaska). This information is important to develop a warning earthquake system. It might be also worth to look at the vertical response of the ground to see if we observe the same behaviour.

2.2 Velocity of the ground according to the location of the events

Still based on S5/S6 data, we can calculate the maximum velocity of an earthquake when it arrives at the site. The calculation of the maximum amplitude is done by the earthquake monitor (see Section 4).

Thus, for both sites LLO and LHO, we generated a world map indicating the location of the earthquakes and the relative velocities seen by each sites, as shown in the appendix A.1.

These plots give a sense of the regions we can break up the events into. Another way to present these results is shown on figure 2 and 3. One plot displays the actual measurements, while the other shows the calculated estimation done with the earthquake monitor. Less events are shown on the first plot because of missing data. This lack of data limits the conclusion that can be made from these sets. We know that the earthquake monitor estimation is good 95% of the time within a factor a 4 (see section 4). Thus, to do a full analysis, we will concentrate our effort on the estimation results. This allows us to separate the earthquakes into three categories.

1. Velocity above 70 μm/s. This usually corresponds to a large magnitude earthquake (7.5+), except when the earthquake is happening less than 4000 kilometres away.
2. Velocity between 30 μm/s and 70 μm/s.
3. Velocity below 30 μm/s. This category contains most of the earthquakes.

Having categories will help us adapt our strategy regarding the interferometers. Tentatively we know that the first category earthquakes will be hard to act on. The second category is a "grey area" right now, and hopefully we will be able to do something about the third category (which regroups most of the events).

As we just did for the ground, the next subsection will present the same work on the interferometers themselves, hoping to find some similar patterns.

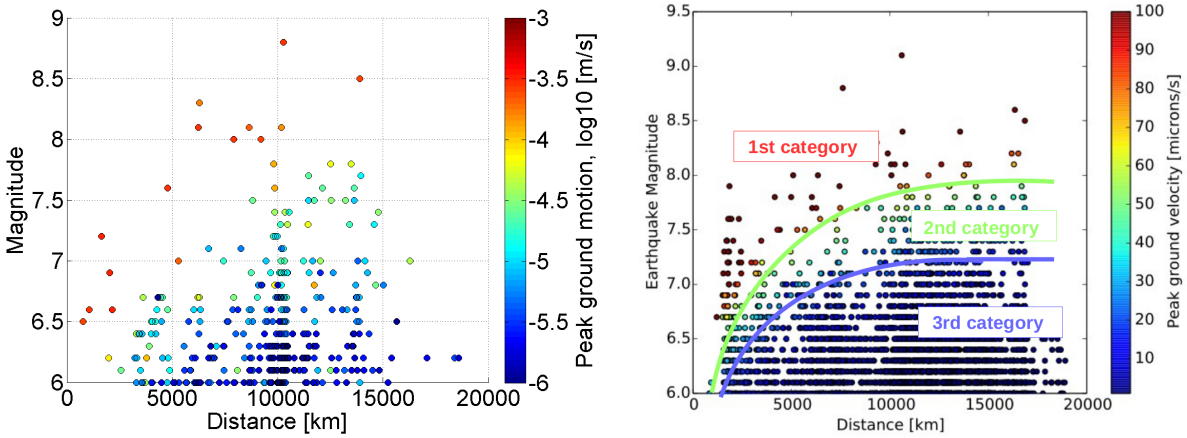

(a) Measured peak ground velocity

(b) Estimated peak ground velocity

Figure 2: Histogram of the earthquakes peak ground velocities at LLO, according to distance and magnitude.

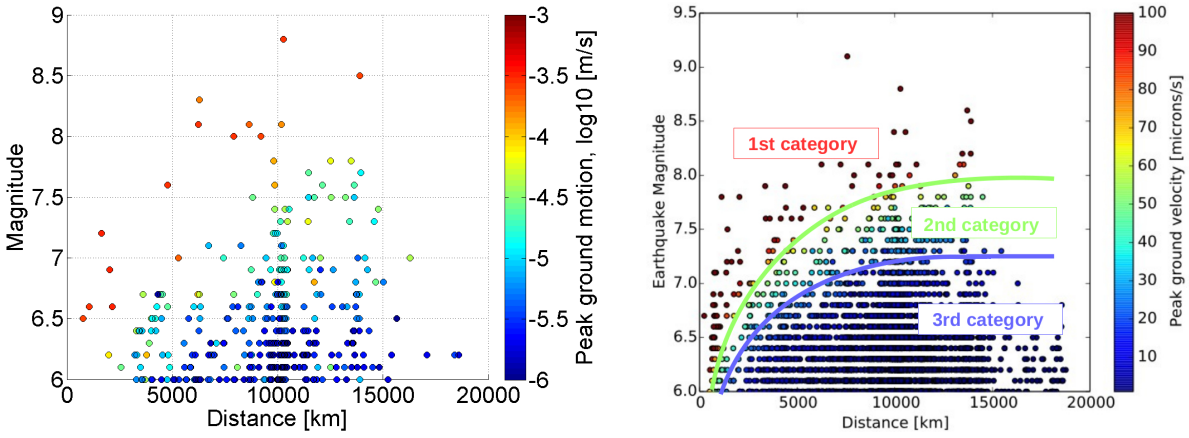

(a) Measured peak ground velocity

(b) Estimated peak ground velocity

Figure 3: Histogram of the earthquakes peak ground velocities at LHO, according to distance and magnitude.

2.3 Interferometers status according the location of the events

The work that has been done in subsection 2.2 on the ground velocity can now be done on the interferometer itself. This section tries to present the correlation between the interferometers status and the earthquakes location/magnitude. Similarly to figures shown in appendix A.1, appendix A.2 shows world maps with all the major events during S5 and S6. In these figures, the green color indicates that the interferometer stayed lock after the earthquake arrival. The red color indicates that the interferometer lost lock in the next 30 minutes after the earthquake arrival. And, similarly to figure 4, we can present the same data in a histogram form.

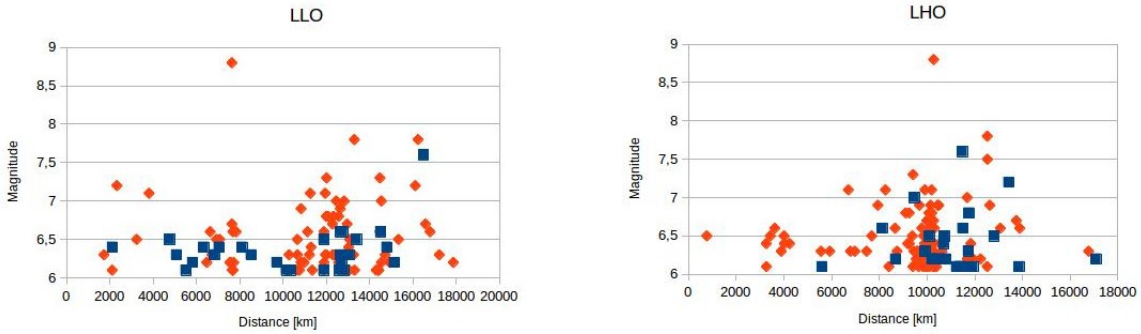

(a) LLO

(b) LHO

Figure 4: Histogram of the interferometers status, according to distance and magnitude of the earthquakes. Blue indicates that the interferometer stayed lock after the event. Red means it lost lock because of the event.

Unlike the ground, we don't see any clear pattern in the interferometers behaviour. This could be explained by several reasons. The main reason is that we assumed that a lock loss that happened after an event is due to the event itself. This is a bold statement that cannot

possibly be true all the time.

S5 and S6 data gave a good overview of the ground behaviour during earthquakes, but without having more information about each of these lock losses, it is hard to draw any conclusions in the interferometers themselves.

3 ER7 data

The analysis during ER7 focuses on the seismic platforms behaviour at both LIGO sites.

3.1 Seismic platform trip status

The detector characterization group has done a complete analysis of the ER7 data ([2]). From May 1, 2015 to June 15, 2015, 21 earthquakes have been observed. Earthquakes are defined as a spike in the 0.03-0.1 Hz LVEA STSB BLRMS above 500 nm/s in at least two degrees of freedom. Six of them made some seismic platforms trip at LLO, Eight at LHO. Figures 5, 6 and 7 show the seismic platforms status during these specific events.

Note: The HEPI platforms at LLO were locked during ER7. Only HEPI status at LHO is shown in this document.

	ITMX-ISI	ITMY-ISI	BS-ISI	ETMX-ISI	ETMY-ISI	HAM2-ISI	HAM3-ISI	HAM4-ISI	HAM5-ISI	HAM6-ISI
EQ May 05 02:00 UTC										
EQ May 07 07:30 UTC										
EQ May 12 07:30 UTC										
EQ May 12 22:00 UTC										
EQ May 29 07:00 UTC										
EQ May 30 11:30 UTC										

Figure 5: Status of the ISI platforms at LLO. The green color indicates that the platform didn't trip during the event. The red color indicates that it did trip. Only unique trips are listed (no trips due to other stages, including SUS)

	ITMX-ISI	ITMY-ISI	BS-ISI	ETMX-ISI	ETMY-ISI	HAM2-ISI	HAM3-ISI	HAM4-ISI	HAM5-ISI	HAM6-ISI
EQ May 05 02:00 UTC										
EQ May 07 07:30 UTC										
EQ May 10 21:45 UTC										
EQ May 12 07:20 UTC										
EQ May 20 23:00 UTC										
EQ May 29 07:00 UTC										
EQ May 30 11:30 UTC										
EQ June 01 20:15 UTC										

Figure 6: Status of the ISI platforms at LHO. The green color indicates that the platform didn't trip during the event. The red color indicates that it did trip. Only unique trips are listed (no trips due to other stages, including SUS)

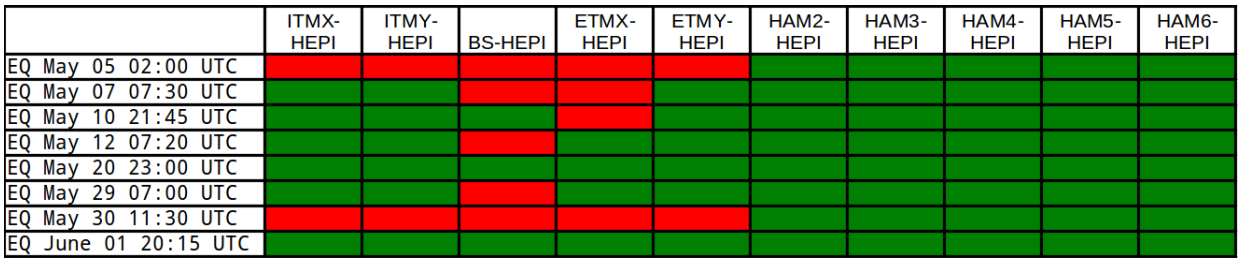

Figure 7: Status of the HEPI platforms at LHO. The green color indicates that the platform didn't trip during the event. The red color indicates that it did trip. Only unique trips are listed (no trips due to other stages, including SUS)

3.2 Nature of the trips

The watchdogs status indicates the nature of each trip. Tables 3 and 4 display the nature of the platform trips for all the trips presented in the previous subsection.

	Stage 1 Actuators	Stage 1 CPS
BSC-ISI	100 %	0 %
HAM-ISI	0 %	100 %

Table 3: Nature of the trips during events at LLO

	Stage 1 Actuators	Stage 1 CPS	GS13
HEPI	100 %	0 %	0 %
BSC-ISI	100 %	0 %	0 %
HAM-ISI	0 %	77.27 %	22.73 %

Table 4: Nature of the trips during events at LHO

3.3 Origin of the trips

Thanks to the Earthquake monitor (see section 4), we know the arrival of the primary, secondary and surface waves. Table 5 shows the correlation these times and the time of the trips.

At both sites, all the trips observed during ER7 happened after the surface waves arrival. This is different form what we observed during S5 & S6 (see section 2), which reinforce the statement that we should focus on recent data to understand the interferometer behaviour.

	LLO	LHO
Trips due to P-waves	0 %	0 %
Trips due to S-waves	0 %	0 %
Trips due to Rf-waves	100 %	100 %

Table 5: Behaviour of the seismic platforms during earthquakes

3.4 Lock status

Looking at the H1:DMT-UP and L1:DMT-UP segments, we can assess on the interferometer lock status during the 21 earthquakes that happened between May 1, 2015 and June 15, 2015. The results presented in table 6 have been made by using the Detector Characterization group Lock webpage (`https://ldas-jobs.ligo.caltech.edu/~detchar/summary/day/20150618/lock/segments/`). We assume that all the lock losses that happened between 0 and 30 minutes after the earthquake arrival are due to the earthquake itself.

	Event	Lock status
ISI trip	May 05 02:00 UTC	No lock
	May 07 07:30 UTC	No lock
	May 12 07:30 UTC	No lock
	May 12 22:00 UTC	No lock
	May 29 07:00 UTC	**Lock loss**
	May 30 11:30 UTC	No lock
No trip	May 1 08:30 UTC	No lock
	May 3 23:30 UTC	No lock
	May 10 01:00 UTC	No lock
	May 10 22:30 UTC	No lock
	May 14 19:35 UTC	No lock
	May 15 17:55 UTC	No lock
	May 19 15:45 UTC	No lock
	May 20 23:00 UTC	No lock
	May 22 22:00 UTC	No lock
	May 24 05:00 UTC	**Lock loss**
	May 24 15:30 UTC	No lock
	May 30 19:30 UTC	No lock
	June 01 07:00 UTC	No lock
	June 01 11:00 UTC	No lock
	June 01 20:30 UTC	No lock
	June 08 07:00 UTC	No lock
	June 10 09:30 UTC	**Lock loss**
	June 11 05:30 UTC	**Lock loss**

	Event	Lock status
ISI trip	May 05 02:00 UTC	No lock
	May 07 07:30 UTC	No lock
	May 10 21:45 UTC	No lock
	May 12 07:20 UTC	No lock
	May 20 23:00 UTC	No lock
	May 29 07:00 UTC	No lock
	May 30 11:30 UTC	No lock
	June 01 20:15 UTC	No lock
No trip	**May 01 08:20 UTC**	**Lock loss**
	May 03 23:15 UTC	No lock
	May 10 01:05 UTC	No lock
	May 12 18:35 UTC	No lock
	May 12 21:25 UTC	No lock
	May 13 16:00 UTC	No lock
	May 14 15:25 UTC	No lock
	May 22 22:00 UTC	No lock
	May 24 15:00 UTC	No lock
	May 30 19:00 UTC	No lock
	June 1 06:55 UTC	No lock
	June 1 10:50 UTC	No lock
	June 12 11:45 UTC	No lock

Table 6: The left table summarizes the events seen at LLO and the right ine the events at LHO

As shown in table 6, the interferometer was not lock for most of the events at both sites. But, from the few events that did happen while the interferometers were locked, we can sat

two things:

1. The interferometer could loose lock even if no seismic isolation platform tripped.
2. Earthquakes made loose the lock on all the observed cases.

The May 29 event is the only example where the seismic platforms trip and the interferometer lost lock LLO. We will study this specific case in the next subsection.

3.5 Study of March 29 event at LLO

This event correspond to a 6.7 Magnitude earthquake in Alaska (5771 kilometres away from LLO). Based on the categories established in subsection 2.2, this earthquake is a category 3.

Looking at seismic data around that period, we can make several observations. These comments are made by observing ITMX and HAM3 around that time. A more consistent study of all the platforms would be necessary to make a stronger statement.

Note: All the time series presented in this subsection are band passed between 0.03 Hertz and 0.1 Hertz.

1. Figure 8 shows that the lock loss of the interferometer happened right at the P-wave arrival time, while the seismic platforms tripped around 30 minutes later.
2. As explained in subsection 3.2, all the BSC-ISI trips are due to the actuators. We can go a step further by saying that it is due to horizontal actuators, as shown in figure 9. For HAM3, the cause of the trip is CPS-H1, as shown on figure 10 (the actuator amplitude signal is around 20,000 counts at that time).
3. The event amplifies the ground and the platforms motion by a factor of ~200 below 2 Hertz, as shown in figure 11 and 12.

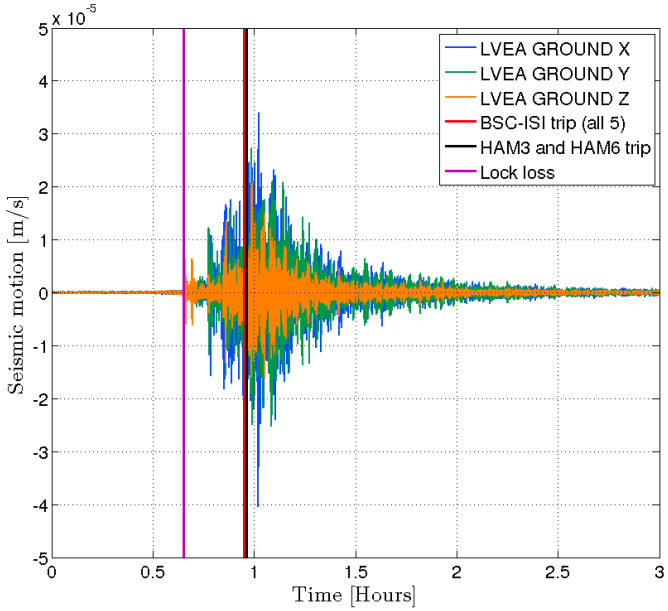

Figure 8: Time series of a LLO ground seismometer. In this example, the interferometer looses lock at the P-wave arrival time while the seismic platforms tripped around 30 minutes later.

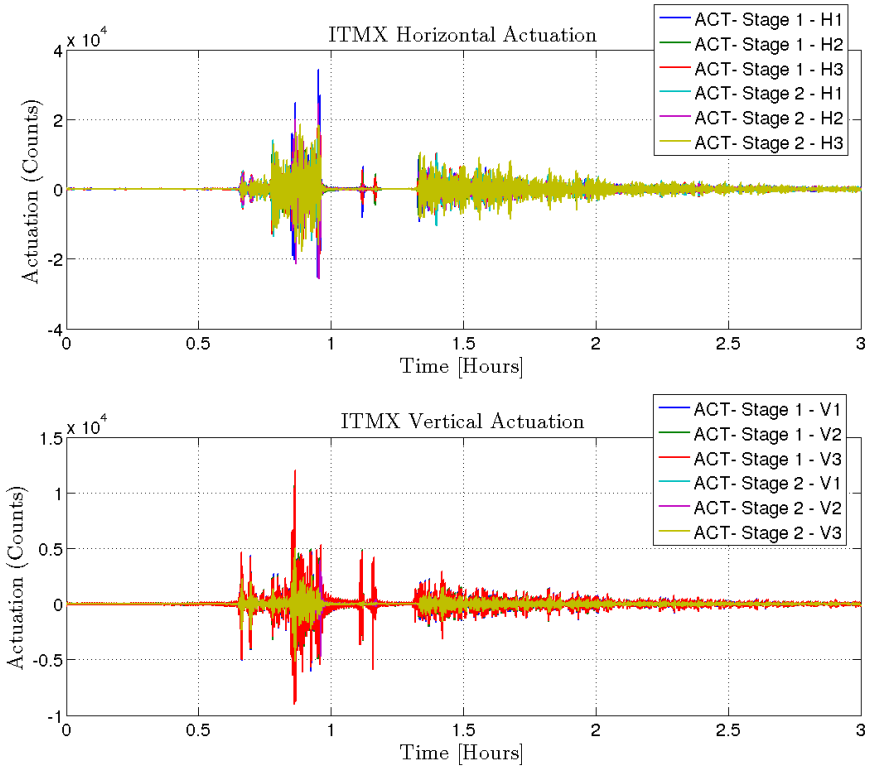

Figure 9: Time series of the ITMX actuators in the local basis. For this event, the trip is due to the actuator H1.

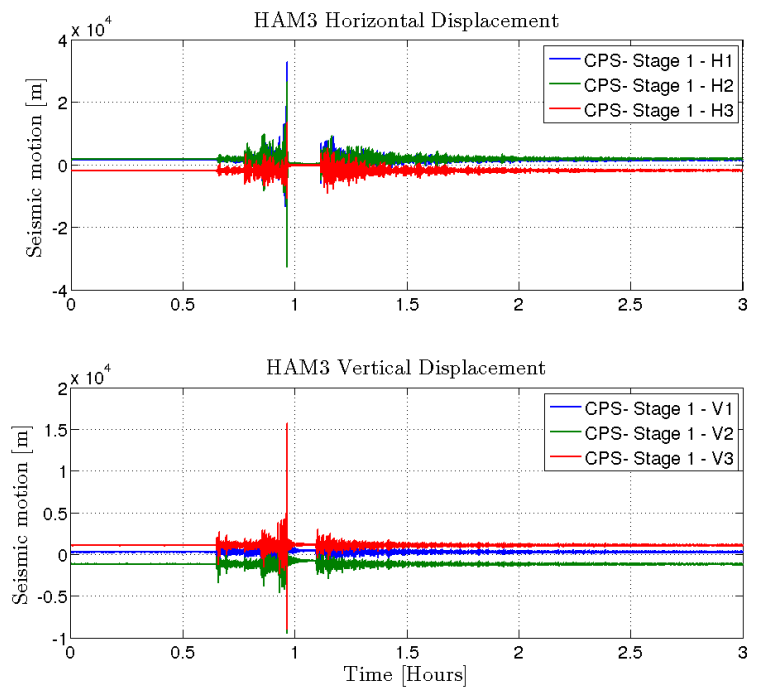

Figure 10: Time series of the HAM3 CPS in the local basis. For this event, the trip is due to the CPS H1.

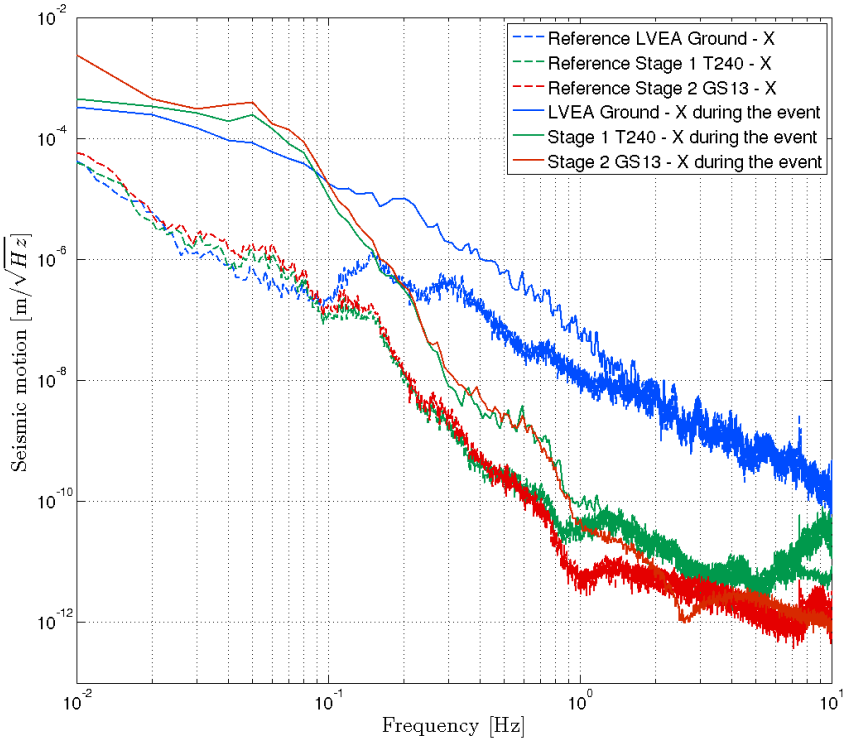

Figure 11: ASD of the ITMX sensors in the X direction. The ASDs of the same signals are shown during a quiet time as a reference: an amplification of ~200 below 2 Hertz is observed

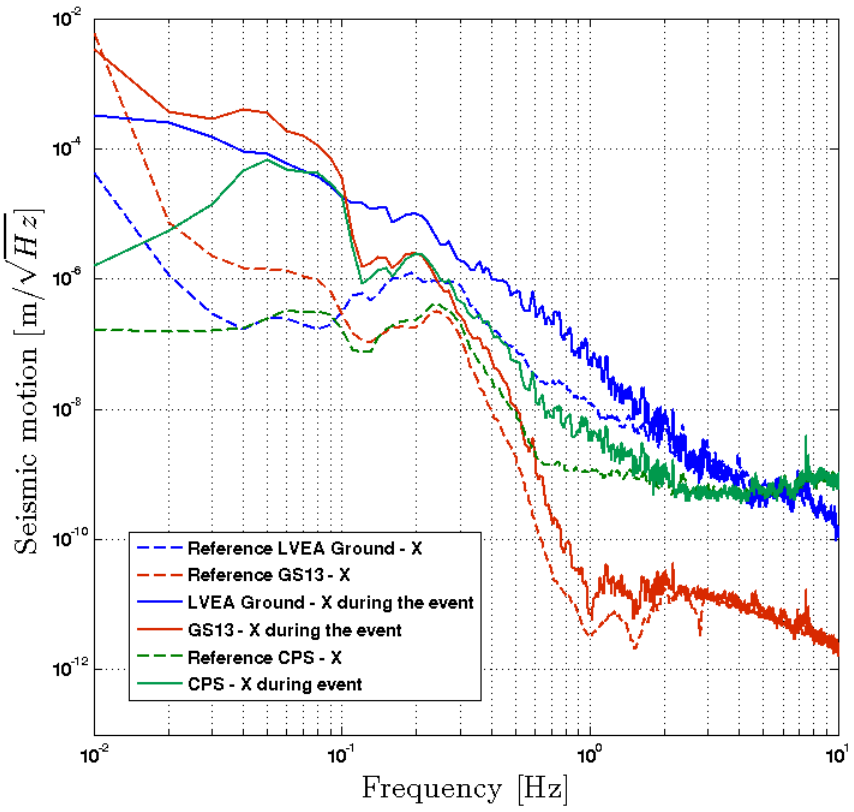

Figure 12: ASD of the HAM3 sensors in the X direction. The ASDs of the same signals are shown during a quiet time as a reference: an amplification of ~200 below 2 Hertz is observed

3.6 Study of June 10 event at LLO

This subsection presents a case where the interferometer lost lock but none of the seismic systems trip. The event is a 5.5 Magnitude earthquake in Japan (10444 kilometres away from LLO). Based on the categories established in subsection 2.2, this earthquake is a category 3.

Looking at seismic data around that period, we can make several observations. These comments are made by observing ITMX and HAM3 around that time. A more consistent study of all the platforms would be necessary to make a stronger statement.

Note: All the time series presented in this subsection are band passed between 0.03 Hertz and 0.1 Hertz.

1. Figure 13 shows that the lock loss of the interferometer happened around the maximum amplitude of the event (surface waves).

2. In this example, despite the increase in the increase of motion, the actuators and sensors are far away from the trip point, as shown in figure 14 and 15. Most of the amplification is horizontal.

3. The event appears as a "bump" around 50 mHz. It amplifies the motion by a factor of ~100 around that frequency, as shown in figures 16 and 17.

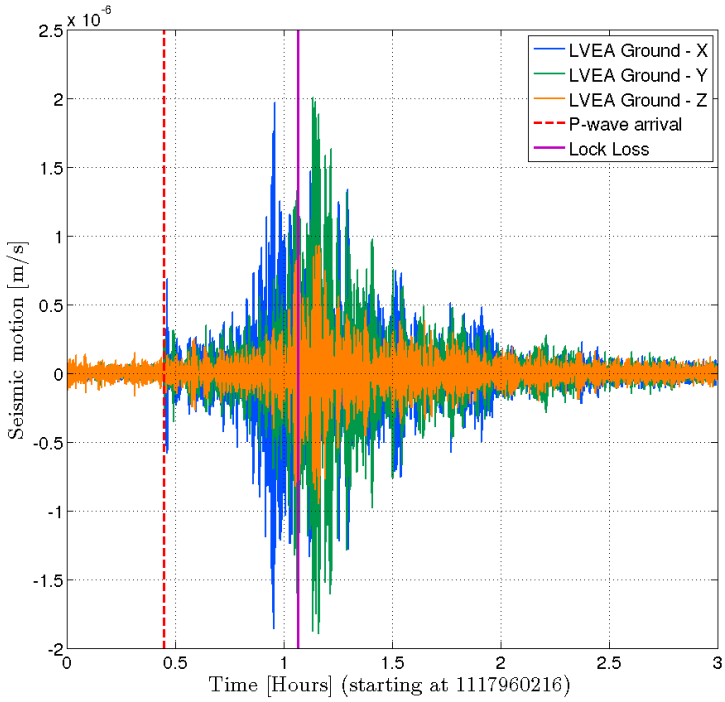

Figure 13: Time series of a LLO ground seismometer. In this example, the interferometer looses lock at the surface wave arrival time.

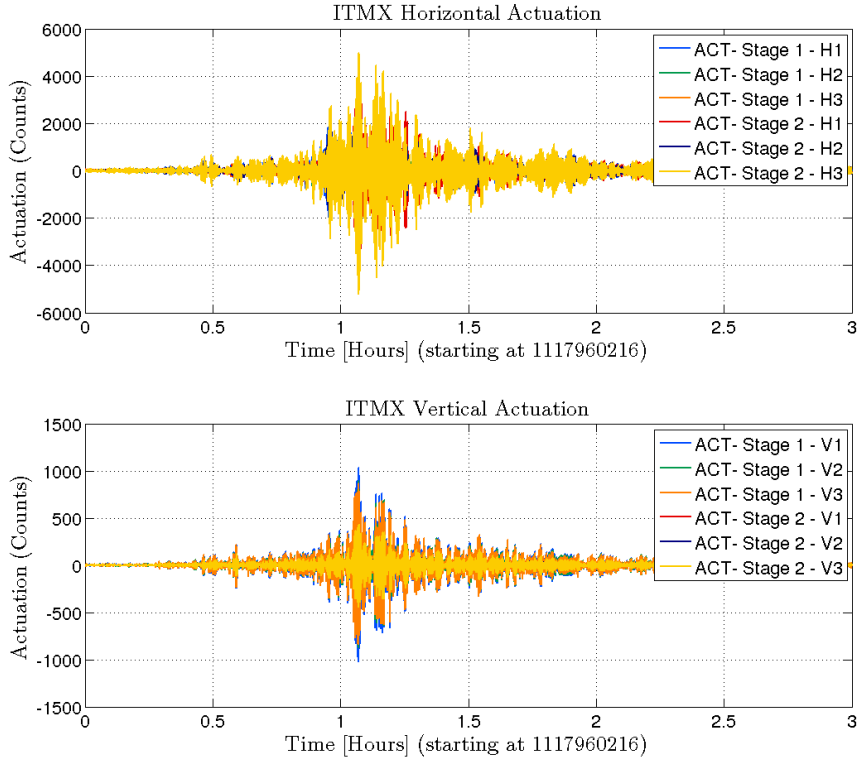

Figure 14: Time series of the ITMX actuators in the local basis.

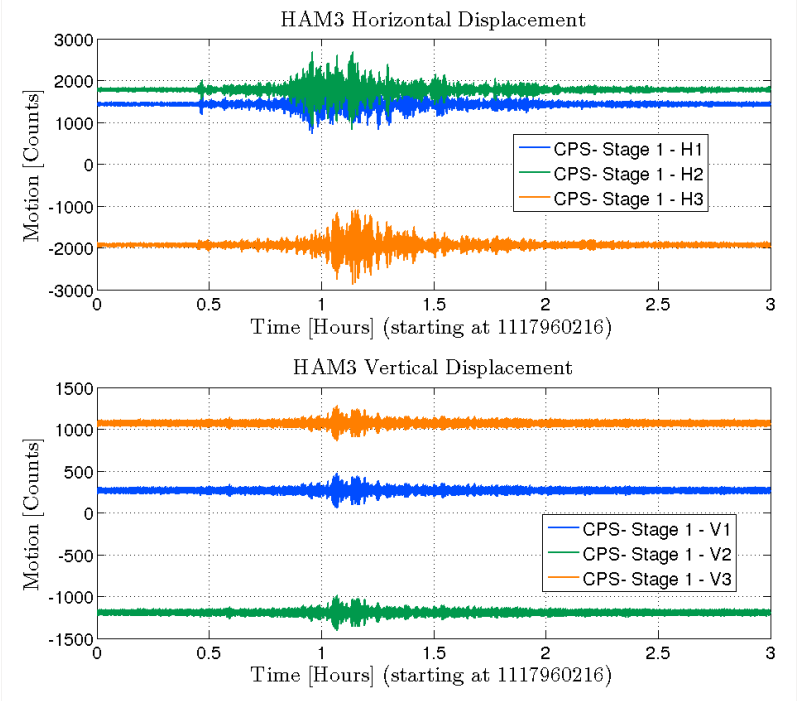

Figure 15: Time series of the HAM3 CPS in the local basis.

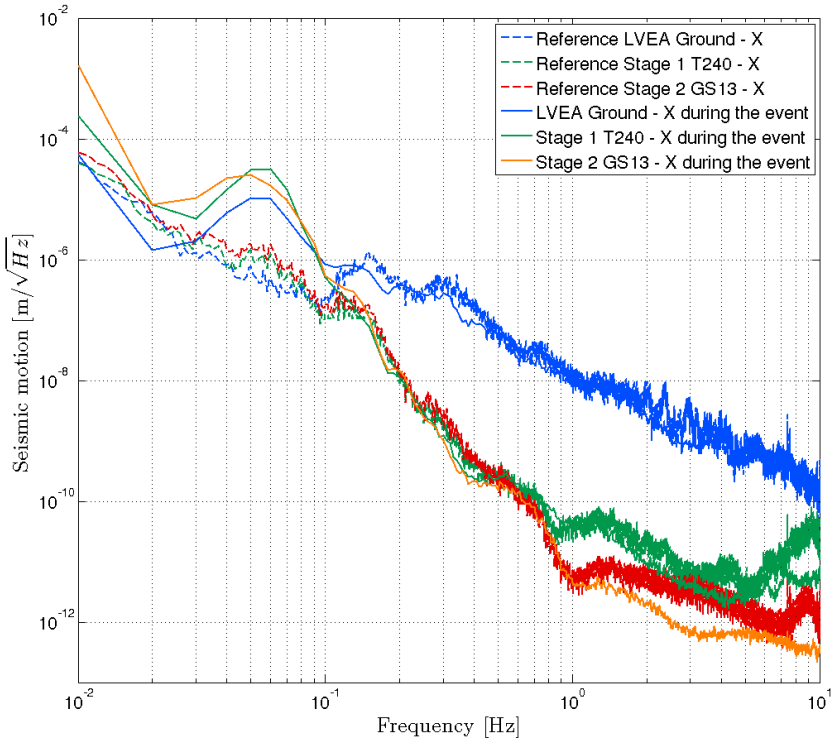

Figure 16: ASD of the ITMX sensors in the X direction. The ASDs of the same signals are shown during a quiet time as a reference: an amplification of ~100 around 50 mHz is observed

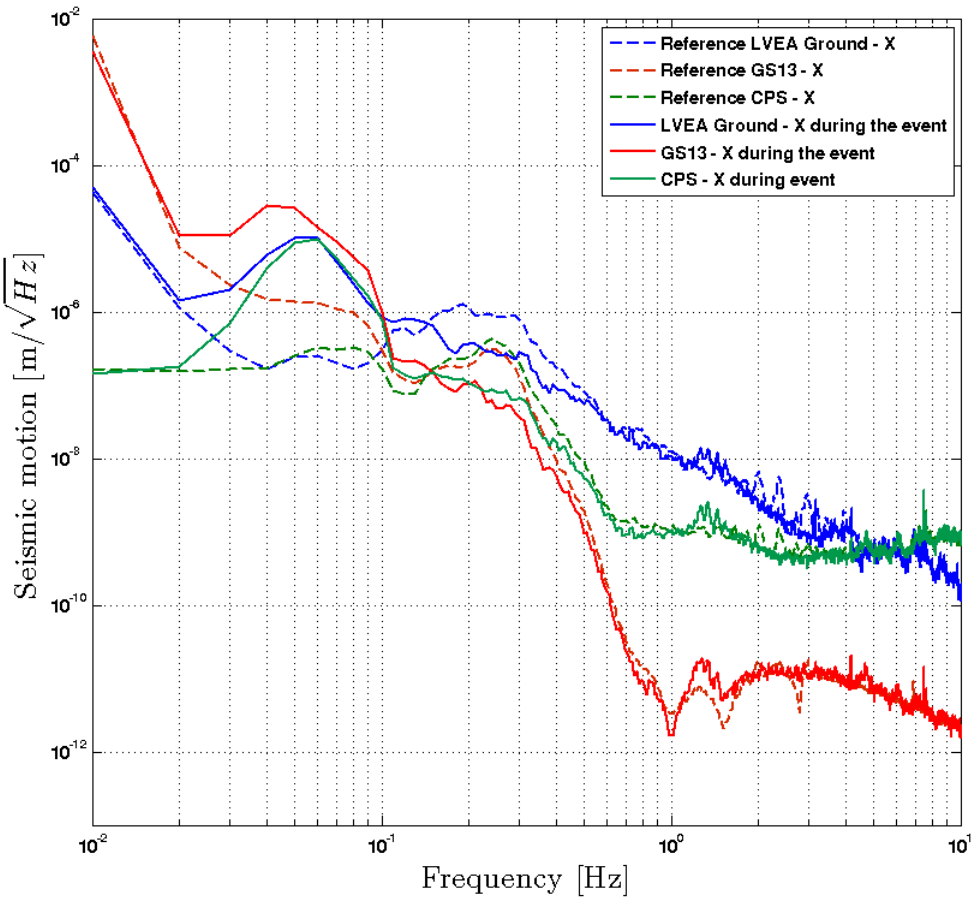

Figure 17: ASD of the HAM3 sensors in the X direction. The ASDs of the same signals are shown during a quiet time as a reference: an amplification of ~100 around 50 mHz is observed

In both of the cases presented, we observed two very different ground behaviours, summarized in table 7. This tells us that the categories defined in subsection 2.2 are not viable. We need to re-assess this previous statement.

	EQ May 29 07:00 UTC	EQ June 10 09:30 UTC
Magnitude and location	6.7 in Alaska	5.5 in Japan
Ground velocity when lost lock	~10 μ/s	~1.5 μ/s
Ground velocity when trip	~30 μ/s	no trip
Corner frequency	2 Hz	100 mHz
Category (according to section 2.2)	3	3

Table 7: Summary of the informations gathered from the two earthquakes sudied in the previous subsections

3.7 Overview of all the events: redefining the earthquakes categories

Based on the observations made before, we know that ISI trips and lock losses are not necessarily related. The goal of this session is to look at all the 24 events from LLO and their ground velocity. The plots are generated using IFO:ISI-BS_ST1_SENSCOR_GND_STS_X_BLRMS_30M_100M.rms channel.

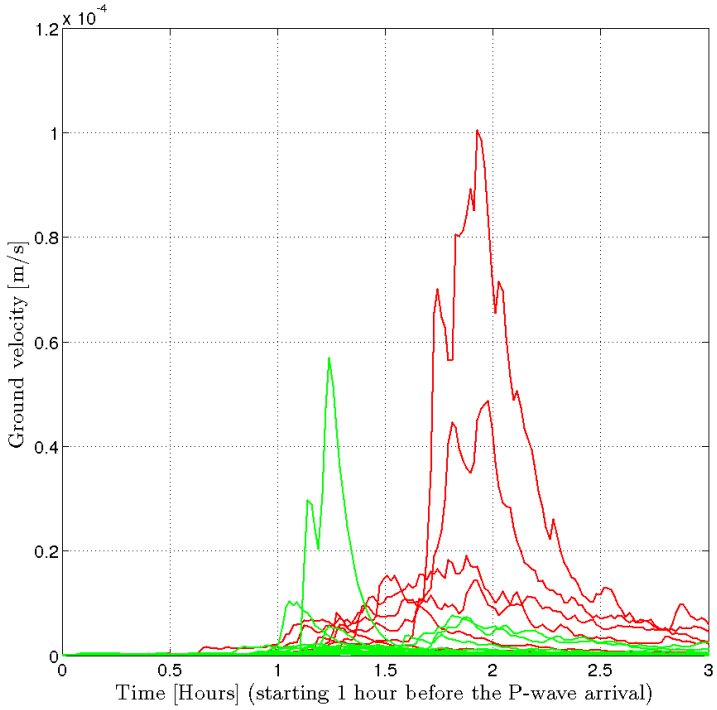

Figure 18: Band Limited RMS of a LVEA ground seismometer in the X direction. All the plots start 1 hour before the P-wave arrival time. Red represents all the events that made some ISI trip, green the event that didn't trip.

As shown in figure 19, the events 16, 23 and 24 made loose the lock of the interferometer even if the ground amplification was not that important (~0.7 μ/s). These events are charactized by creating an amplification around 50 mHz. Also, all the ISI trips happened for a ground velocity greater than 8 μ/s (except for event 11).

Thus, there is no obvious pattern in the interferometer behaviour. But, it seems that there

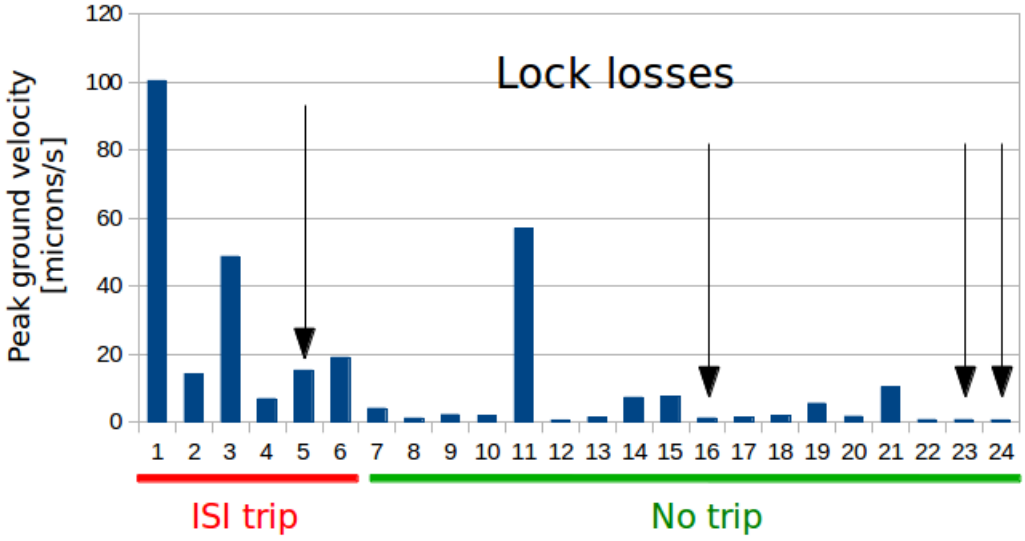

Figure 19: Maximum ground velocity per event.

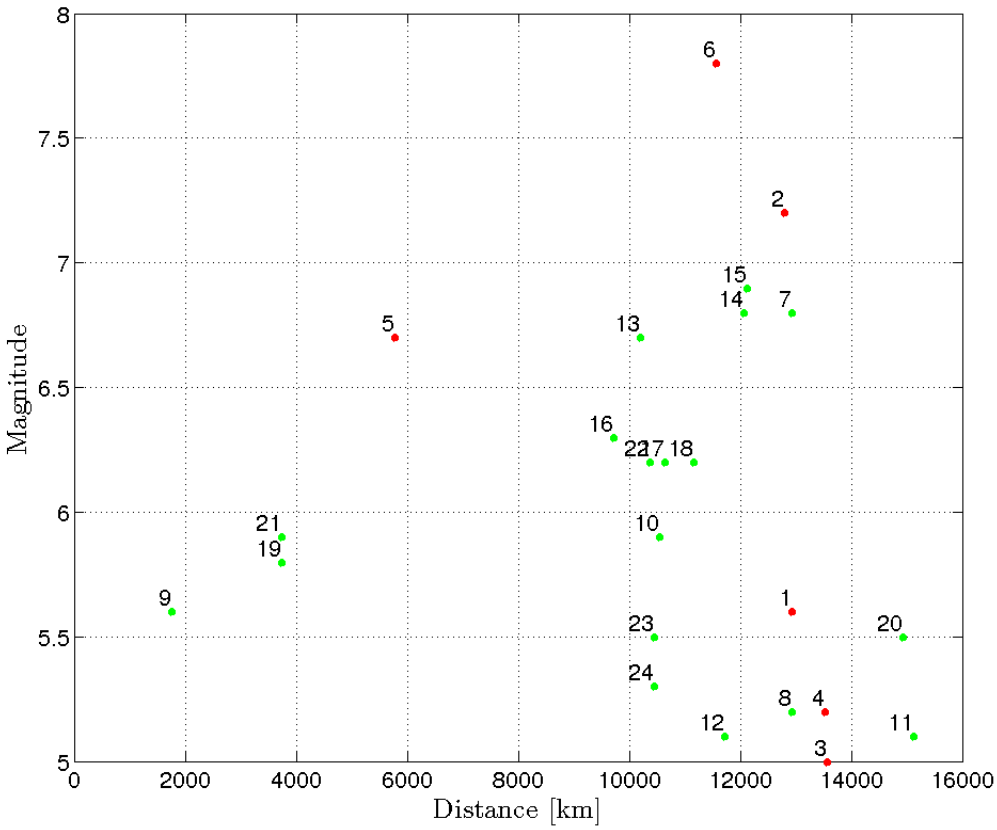

Figure 20: Relative Magnitude/Distance for the 24 events

is a threshold around 8 μ/s. I would re-asses the categories in this manner:

- 0μ/s$\leq$EQ$\leq$0.6μ/s: Very unlikely to trip the ISI or to loose lock.

- 0.6μ/s≤EQ≤8μ/s: Very unlikely to trip the ISI, but the interferometer would probably loose lock.
- 8μ/s≤EQ: Would probably trip the ISI and loose lock.

These categories are bold, but it is a start. I hope we will reajust this statement by having more and more data, mostly thank to the Earthquake webpage (see section 4.5).

4 Seismon

This section describes the functions for Seismon, developed to mitigate the effects of teleseismic events on ground-based interferomic gravitational wave detectors. It uses event notices received from USGS and makes time of arrival and amplitude predictions are made for earthquake seismic wave phases at sites of current detectors. Using a combination of earthquake magnitude, distance, and depth information, a prediction of the likelihood of the earthquake causing data disruption at the sites is made.

Gravitational-wave detectors are susceptible to significant seismic motion near the detectors. Seismic motion from human activity near the sites, from wind and from ocean waves are among the most common sources of these disturbances. Earthquakes, due to the ground motion they induce, also effect $h(t)$. During the last LIGO science run, large amplitude earthquakes from around the world would typically cause the detectors to fall out of lock. Not only was the data around the time of the earthquake not useful for GW detection, but it would also take a significant amount of time for the detectors to return to the locked state. With knowledge that an earthquake of significant magnitude was about to arrive, scientists on site could take preventative measures to limit the amount of downtime the detectors experienced. To facilitate this, we have developed seismon, a software package designed for autonomous notification of teleseismic events likely to affect GW detectors.

In the following, we describe how Seismon works.

4.1 PDL Client

There are three sources of event notifications which seismon uses for analysis. The first is public notifications distributed by USGS in GeoJSON format at `http://earthquake.usgs.gov/earthquakes/feed/geojson/all/hour`. This file is downloaded every 5s and parsed for new events. The second is events from the IRIS database.

The third are the type we concentrate on here. These are private notifications distributed for observatory use through USGS's Product Distribution Layer (PDL), which has been configured to receive all notifications of earthquakes worldwide. These messages are in the form of either EQXML or QuakeML Extensible Markup Language (XML) files.

Documentation can be found in `http://ehppdl1.cr.usgs.gov/index.html#documentation`. The source code can be found in `http://ehppdl1.cr.usgs.gov/ProductClient/ProductClient.jar`. It can be called like the follows:

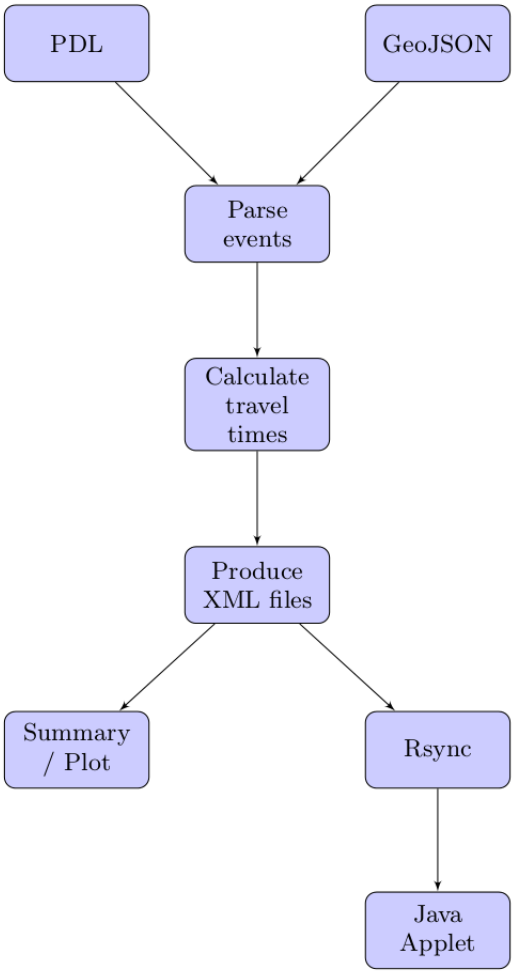

Figure 21: A flow chart of the Seismon pipeline.

java -jar ProductClient.jar –receive –configFile=config.ini ProductClient.jar can be attained from the link in the footnote. An example config.ini file can be obtained from the Seismon github at `https://github.com/gwpy/seismon/tree/master/` in the input directory. The only change necessary is modifying the XML output directory from the defaults to where you desire. What the various options mean can be found in the ProductClient documentation.

In the output directory specified, directories will be created and populated with the xml files. The directory will be named for the ID string assigned by the PDL. An example is ak10885303. The subdirectories will contain a UTC timestamp corresponding to when the notice was sent to the PDL (there can be multiple of these as magnitudes and locations are improved). An example xml file in this sub-directory is xml/ak10885303-1070469866_eqxml.xml. It contains location, magnitude, time, and other information.

4.2 PDL Client: What is required to run / who it communicates with

As far as I can tell, java is the only requirement. It communicates with a server maintained by the USGS observatories. We are just listening in on the messages sent from the observatories,

we do not send any information back.

4.3 PDL Client: What it does / what it outputs

The second step of the process is to convert event notifications to information about the time of arrival and amplitudes at the sites. The event notification pipelines produce earthquake information including time, latitude, longitude, depth, and magnitude. The first step is to make time-of-arrival predictions at the sites. Using the iaspei-tau package [1] wrapped by Obspy [2], travel times for the P and S wave components are calculated. An approximate arrival time for the surface waves are calculated assuming a constant 3.5 km/s speed value.

The second step is to make amplitude predictions for each site. We estimate the amplitude of the surface waves, Rf_{amp}, at the sites using the equation

$$Rf_{amp} \propto \frac{M}{\sqrt{d}} * e^{-2*pi*h*f_c/c} \quad f_c = 10^{(5.3-M)/3} \tag{1}$$

where M is the magnitude of the earthquake, d is the distance, h is the depth of the earthquake, c is the speed of the surface-waves, and f_c is the corner frequency. This was developed as a fit to S5 and S6 earthquakes at LHO and LLO.

These are wrapped in Seismon in seismon_traveltimes, which is in the bin directory in github. It takes a parameter file, in example of which is in the input/ directory, which directs the output of the code. The arguments it takes are start and end GPS times, the parameter file, and the type of XML file being analyzed. An example command is

The –doPrivate flag corresponds to the PDL client, –doPDL corresponds to the JSON files, and –doIRIS accesses the IRIS database. It outputs XML files with the above information for each current GW interferometer. In the output directory specified, the xml files will appear. The code loops through the XML files from the first step and finds those between the start and end GPS times specified. It creates XML files with the naming structure ID-GPS.xml. An example xml file in this sub-directory is xml/ak10885303-1070469866.xml. It contains location, magnitude, time, and other information provided by the original EQXML file, in addition to Rfamp, which is the predicted amplitude in m/s at the site in question, Distances, which corresponds to the distance between the earthquake and site in meters, Ptimes, which is the expected P-wave arrival, Stimes, which is the expected S-wave arrival, and RthreePointFivetimes, which is the expected surface wave arrival time assuming a surface wave velocity of 3.5 km/s.

4.4 What is required to run

The code is in python. I use version 2.6, which is on the clusters.

The packages that probably require installation are:

1. lxml: XML reading and writing.
2. GWpy: maintained by Duncan Macleod, seismon is based off of it

3. lal/glue: for segment manipulation and time-series analysis and the like (required for GWpy)

4. ObsPy: calculate travel times

4.5 Earthquake webpage

Work in progress. In the meantime, please find some informations in S. Biscans DCC page [4].

5 Earthquake Strategy

Work in progress. In the meantime, please find some informations in S. Biscans DCC page [4].

A Appendices

A.1 World maps - Velocity

A.2 World maps - Velocity

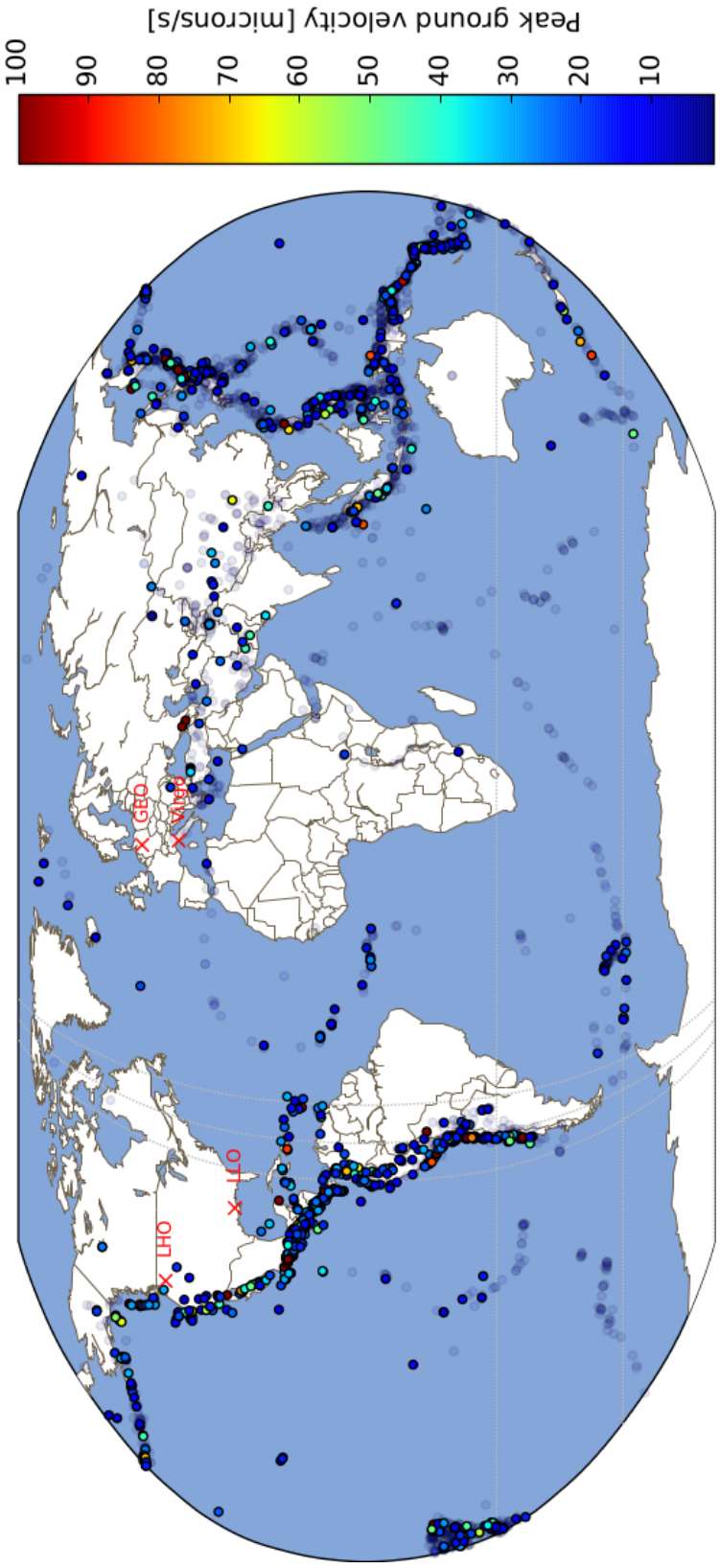

Figure 22: This map indicates the location of all the earthquakes during S5/S6. The color scale corresponds to the linked maximum velocity seen at LLO

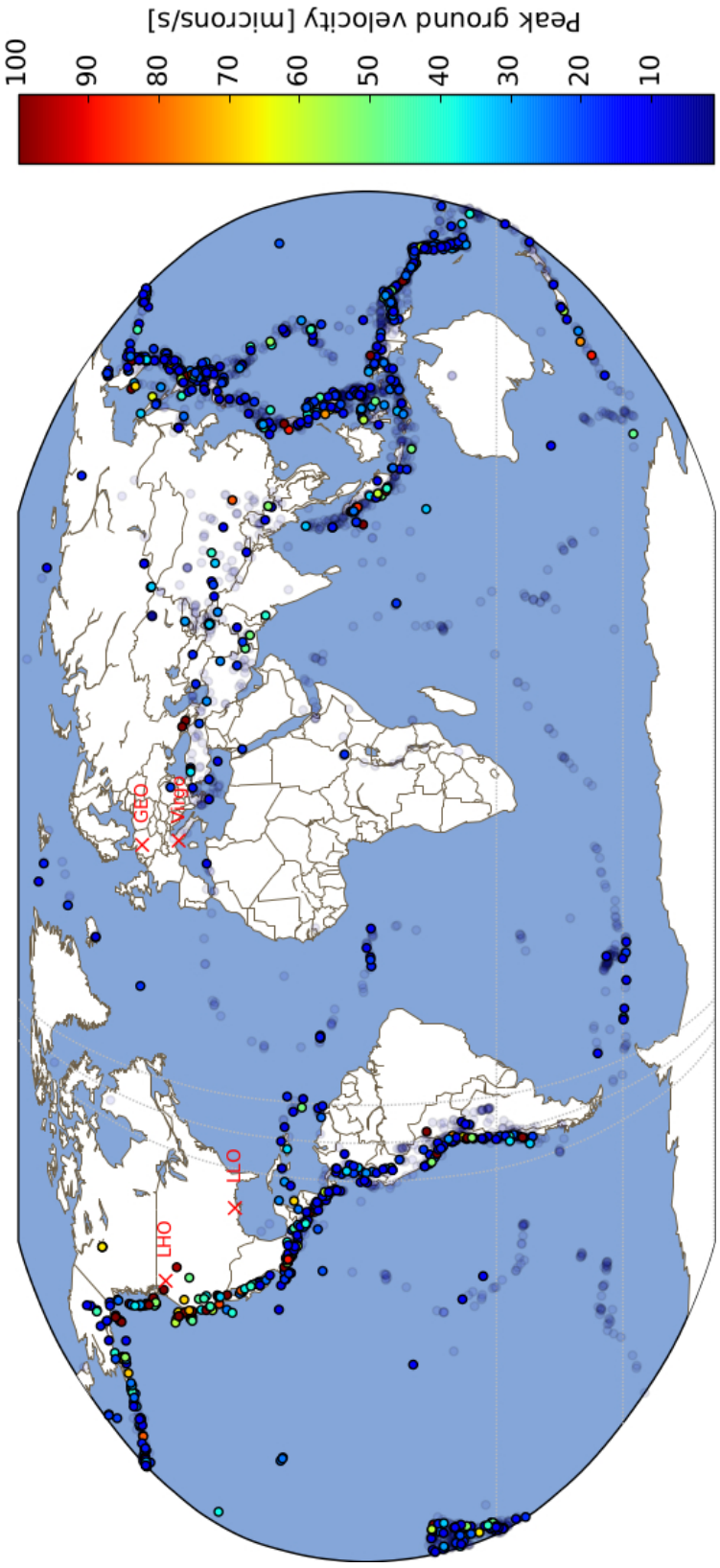

Figure 23: This map indicates the location of all the earthquakes during S5/S6. The color scale corresponds to the linked maximum velocity seen at LHO

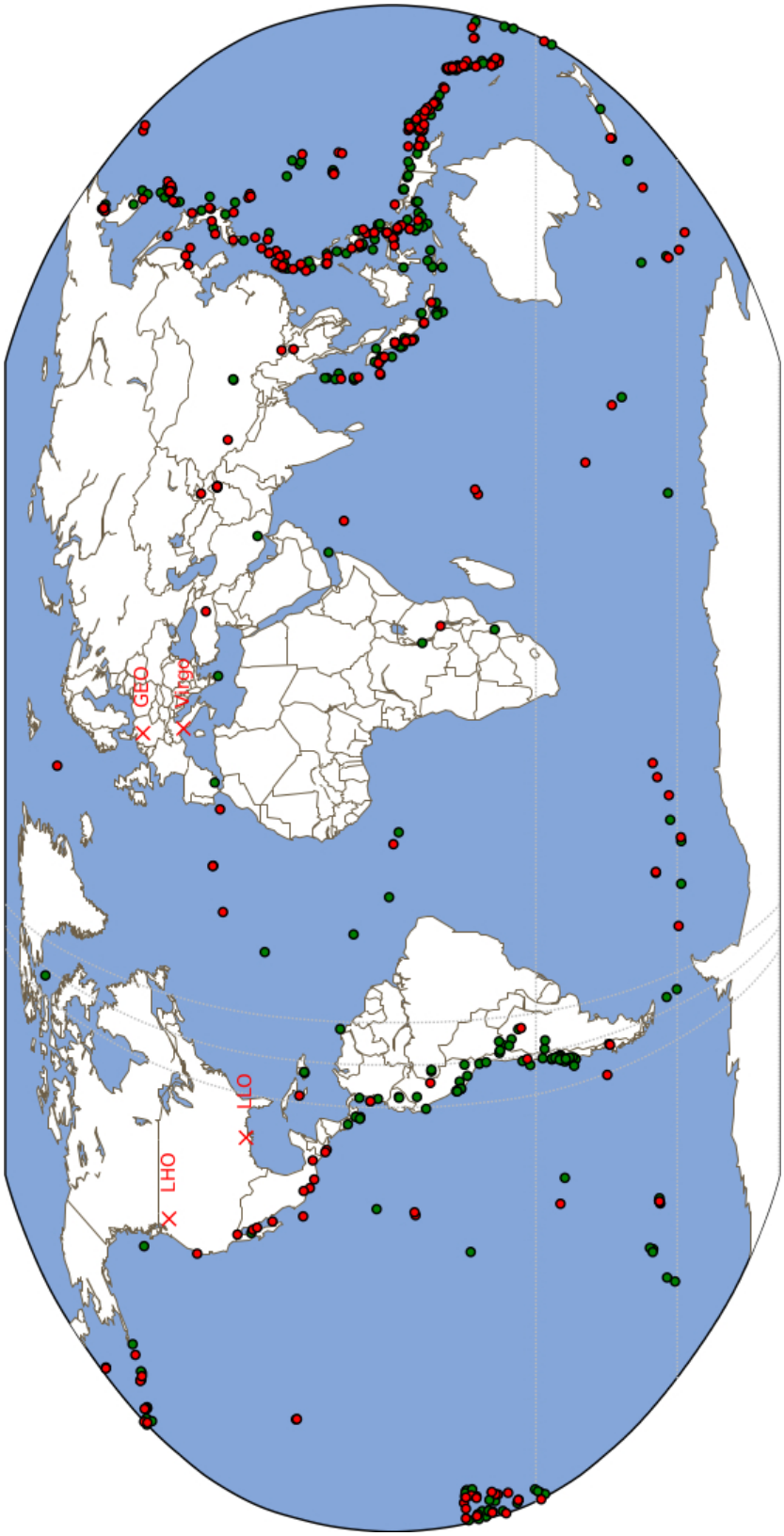

Figure 24: LLO status compared to major earthquakes during S5/S6

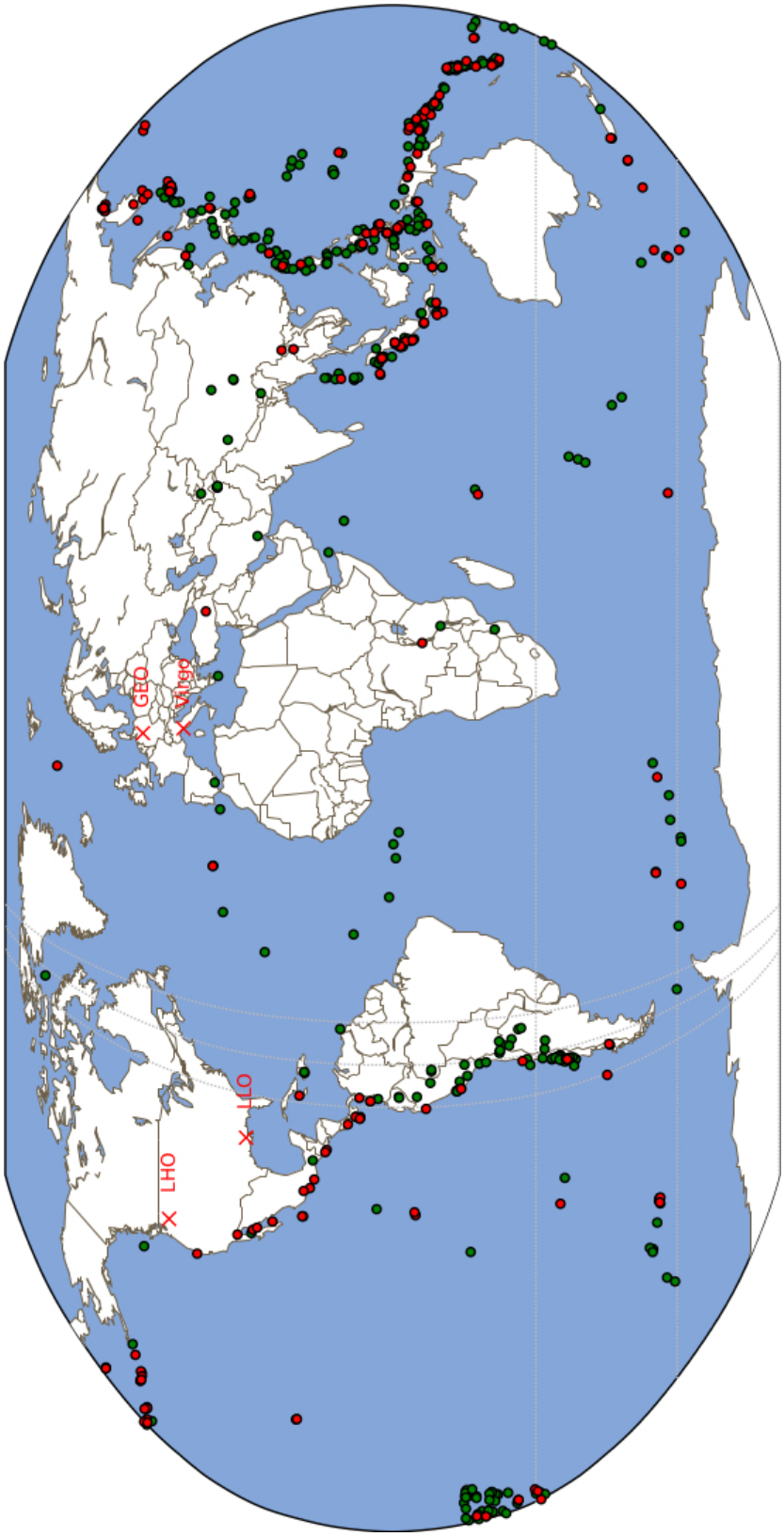

Figure 25: LHO status compared to major earthquakes during S5/S6

References

[1] Jan Harms, T1500266-v1, earthquake lock loss during S5/S6. 28 May 2015, https://dcc.ligo.org/LIGO-T1500266

[2] Jessica McIver, G1500811-v1, ER7 report on DetChar SEI. 19 June 2015, https://dcc.ligo.org/G1500811

[3] Michael Coughlin, G1400811-v3, earthquake monitoring for aLIGO. 25 Aug 2014, https://dcc.ligo.org/LIGO-G1400811

[4] Sebastien Biscans, G1500562-v2, LIGO/VIRGO earthquake studies and controls configurations. 25 Aug 2014, https://dcc.ligo.org/LIGO-G1500652

References

[1] Snoke J.A. Traveltime tables for iasp91 and ak135. *Seismological Research Letters*, 80(2):260–262, 2009.

[2] Moritz Beyreuther, Robert Barsch, Lion Krischer, Tobias Megies, Yannik Behr and Joachim Wassermann. Obspy: A python toolbox for seismology. *Seismological Research Letters*, 81(3):530–533, 2010.